Airfoil Dynamics: Understanding Lift and Drag with Force and Moment Balance Methods

Course: 341B

Henry Glover

Abstract

The aim of this experiment is to compare two separate methods for evaluating both lift and drag forces acting on an a NACA0010 airfoil at an initial and steady velocity of 10 m/s and 20 m/s.

The experiment was conducted within a wind-tunnel, with data acquisition facilitated by a pitot tube transversing across the airfoil connected to VI software on a lab bench. To predict the type of flow the airfoil exhibited a Reynold's number was calculated to characterize the inertial and viscous forces within the flow. The two Reynold's numbers were calculated to be 61,200 ± 1,100 at 10 m/s and 122,000 ± 600 at 20 m/s. Furthermore, the angle of attack on the airfoil was varied and both the lift and drag forces were measured using a pitot tube. Employing the force and balance methods for the analysis of lift and drag lead to confident results. The results showed that an increase in Reynolds number indicated a faster, more turbulent flow. Thus, at a high Reynolds number, the inertial flow is greater than the viscous flow and drag was slightly decreased. Boundary layer thickness may have also contributed to a higher Reynolds number because a thinner boundary layer could cause more turbulence. Using the force balance method, The Lift and Drag plot demonstrated the difference in the efficiencies of Reynold's number at different velocities. The percent error and general trend line for the efficiency plot was indicative of a very small coefficient of drag leading to an increased efficiency. On the other hand, the momentum balance plots were more accurate, steady, and indicative of the efficiency of a greater Reynolds number but failed to capture larger drag coefficients. Both the methods were compared in the following report.

Intro

Airfoils are aerodynamic shapes that are characterized by several parameters. These parameters include **chord length (c):** the length between the leading edge and the trailing edge, **thickness**: the distance between two of the airfoil surfaces, **angle of attack ($\boldsymbol{\alpha}$):** the angle the airfoil is pointed at initial flow, **boundary layer thickness**; the thin layer of fluid adjacent to the airfoil surface, **Reynolds number**; dimensionless parameter to characterize the inertial and viscous flow, and **aspect ratio**; the ratio of the length of the wing to the chord length. Airfoils lift and drag can be characterized in the following general equation below.

$$[L, D] = f(U_0,\ \alpha) \quad (1)$$

Where the Reynolds number can be expressed as

$$Re = \frac{ul}{v} \quad (2)$$

Where *u* is the velocity, *l* is the length, and *v* is the kinematic viscosity of the fluid at room temperature (20 C). To compute lift, an equation was derived to represent the dimensions of the airfoil as expressed in the questions below.

$$C_L = \frac{L}{\frac{1}{2}\rho U_0 S} \quad (3)$$

Where U_0 is initial velocity of the fluid and *S* is the surface area of the wing computed using the chord length *(c)* and span *(b)* of the airfoil. The equation is shown below.

$$S = b * c \quad (4)$$

To compute the dimensionless coefficient of drag a similar equation is derived shown below.

$$C_D = \frac{D}{\frac{1}{2}\rho U_0 S} \quad (5)$$

To calculate for an approximation of drag using the momentum balance, a new set of equations are derived. The presence of an airfoil disturbs the streamlines and flow, leading to changes in the velocity profiles. Thus, the momentum balance equations allow for the analysis of the wake velocity caused by the reaction forces from the airfoil. The momentum balance utilizes Newton's first law of physics.

$$\vec{F} = \frac{d(m\vec{v})}{dt} \quad (6)$$

A continuity equation is then used to satisfy the conservation of mass and integrated as shown in the expression below

$$\rho \int_{-\infty}^{\infty} u_1(y)dy + \frac{dm'}{dt} + \rho \int_{-\infty}^{\infty} u_2(y)dy = 0 \quad (7)$$

where *(ρ)* is the density of the fluid and m' represents the net mass flux per unit span. An assumption is made that the fluid flow is constant and incompressible. Thus, velocity was measured with the u components to solve for drag *(D)*.

$$D = \frac{\rho U_0 A}{h} \int_{-\frac{h}{2}}^{\frac{h}{2}} \left[\frac{u_w(y)}{U_0} - \left(\frac{u_w(y)}{U_0} \right)^2 \right] dy \quad (8)$$

The momentum thickness of the wake velocity is defined in the following equation below.

$$\theta = \int_{-\frac{h}{2}}^{\frac{h}{2}} \left[\frac{u_w(y)}{U_0} - \left(\frac{u_w(y)}{U_0} \right)^2 \right] dy \quad (9)$$

Where θ is the momentum thickness. The formula is then simplified and substituted into the experiment as shown in the expression below.

$$D = \rho U_0^2 b\theta \quad (10)$$

And

$$C_D = \frac{2b}{S}\theta = \frac{2}{c}\theta \quad (11)$$

Methods and Materials

Using a wind-tunnel, a NACA0010 was placed in the center of two reference pitot tubes. The angle of attack was varied and multiple trials, over the span of a week, were conduction using the initial velocities of 10 [m/s] and 20 [m/s]. The results were processed using LABVIEW VI software. An experimental setup is shown in the figure below.

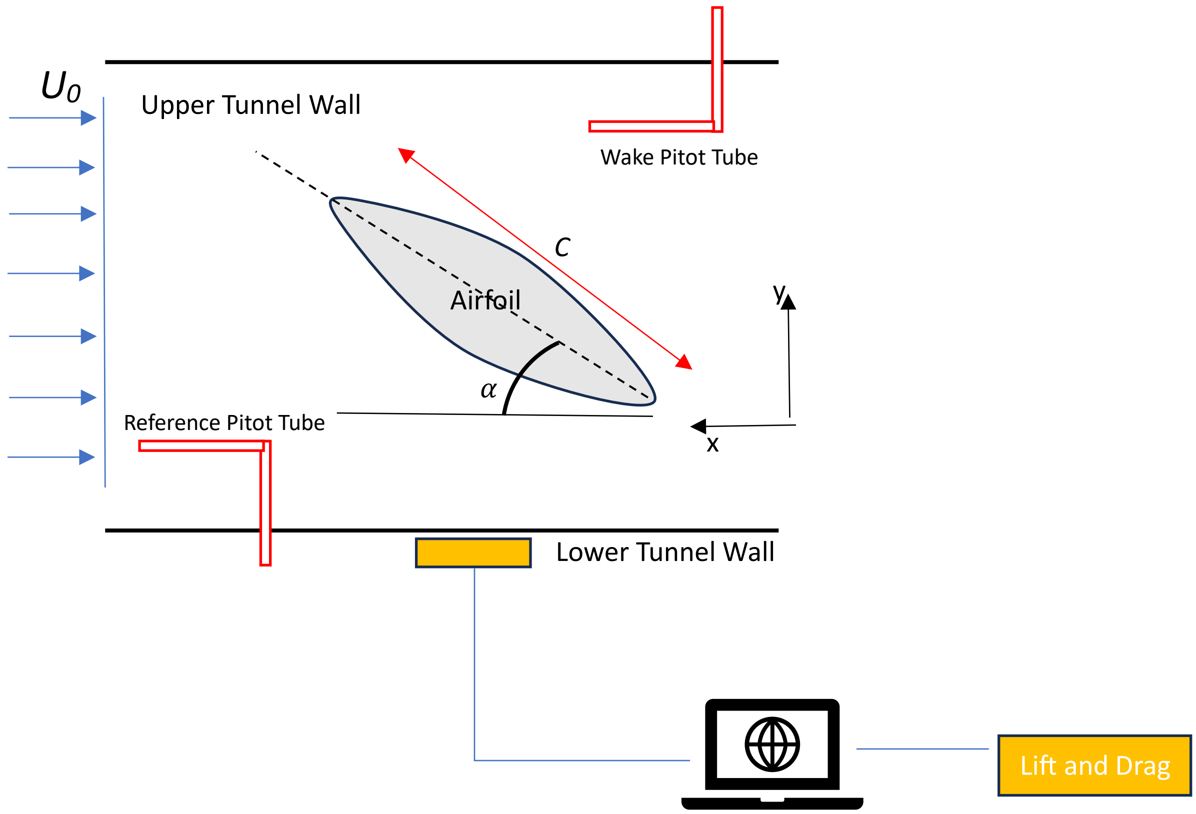

Figure 1 – Experimental setup of inside the wind-tunnel.

The presence of an airfoil in a uniform flow result in a wake velocity profile. This profile is depicted in the figure below and can help visualize the rationale for using the momentum balance approach.

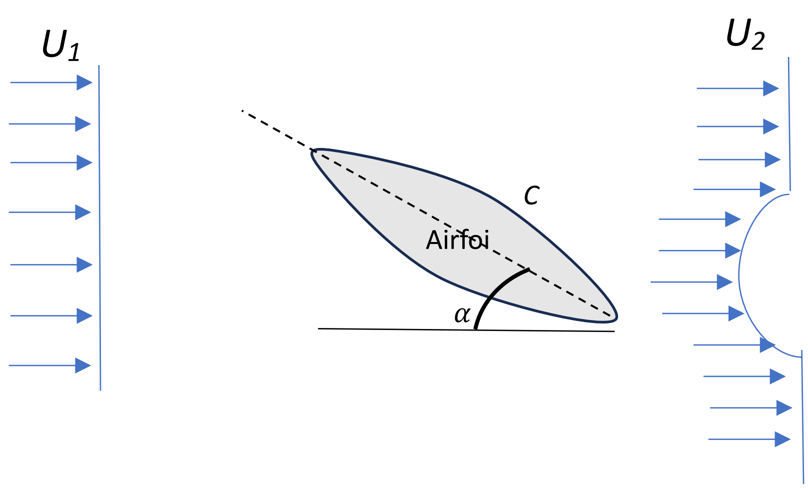

Figure 2- Display of the wake velocity profile caused by the airfoil disturbance.

Results

The force balance and momentum balance approach were calculated using given parameters which included density (ρ), Kinematic viscosity (v), airfoil wingspan (b) and airfoil chord length (c). The given quantities are shown below.

ρ [kg/m^3]	1.205		
v [m^2/s]	0.000015		
b [m]	0.458	±	0.002
c [m]	0.0915	±	0.005

Chart 1 – Given parameters for calculations.

The Reynolds number was then calculated for each initial velocity, 61,200 ± 1,100 at 10 m/s and 122,000 ± 600 at 20 m/s. The force balance was then plotted to display a relationship. In the lift vs. angle of attack plot, an increase in the angle of attack displayed an increase in the lift which indicated the airfoils non-symmetric shape. It is important to note than at an increased Reynolds number, lift increase. This meets the expectation of the scientific assumptions. That being said, more trials of data at different angles of attack would be helpful in characterizing the lift trendline.

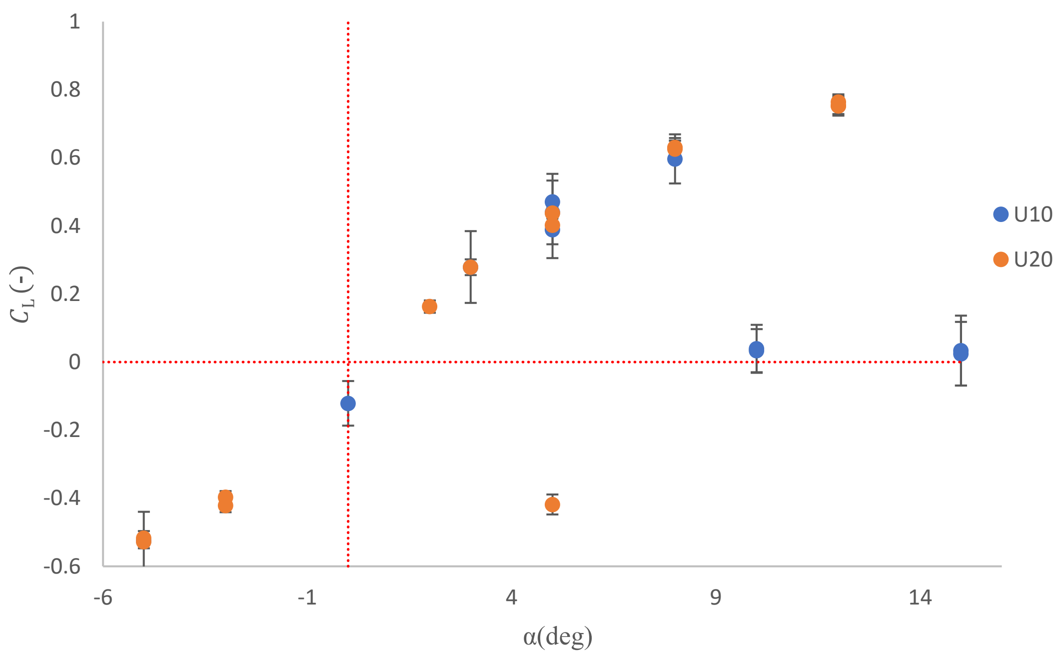

Figure 3 – Coefficient of lift plotted against angle of attack at the initial velocity of 10 [m/s] and 20 [m/s]. The higher velocity displays greater lift even with uncertainties.

Furthermore, in the drag coefficient plot, our expectations are not met. This could be due to the lack of data in the trial set where not enough angles of attack were measured. The assumption is that as Reynolds number increases drag should as well. The plot also displays a bluff drag in the values before the zero value.

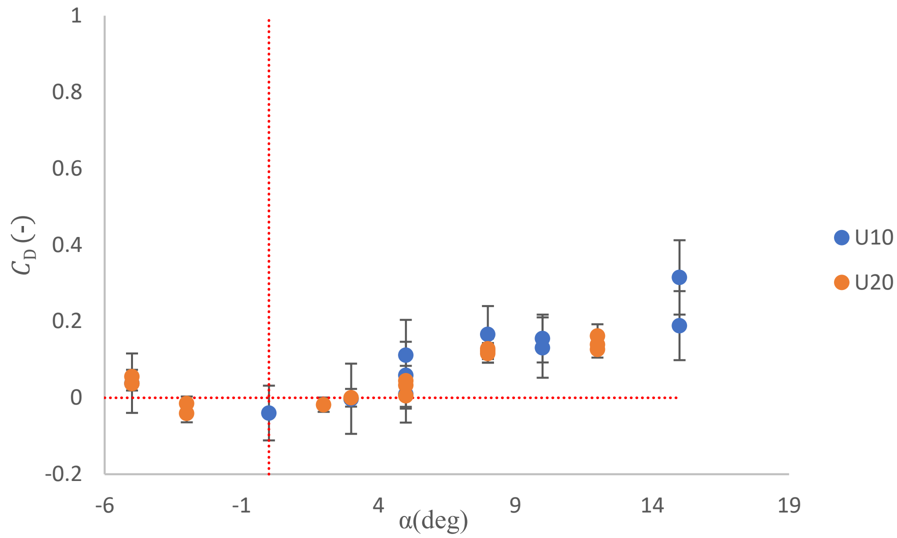

Figure 4 – Skewed results as a higher velocity is indicative of a greater amount of drag. Negative drag coefficients were also not expected nor predicted.

The lift vs. drag plot although messy, aligns with the expectations and demonstrates a set symmetry within uncertainty across the y-axis. As lift increases, drag increases and at a higher Reynolds number, there is more lift and drag.

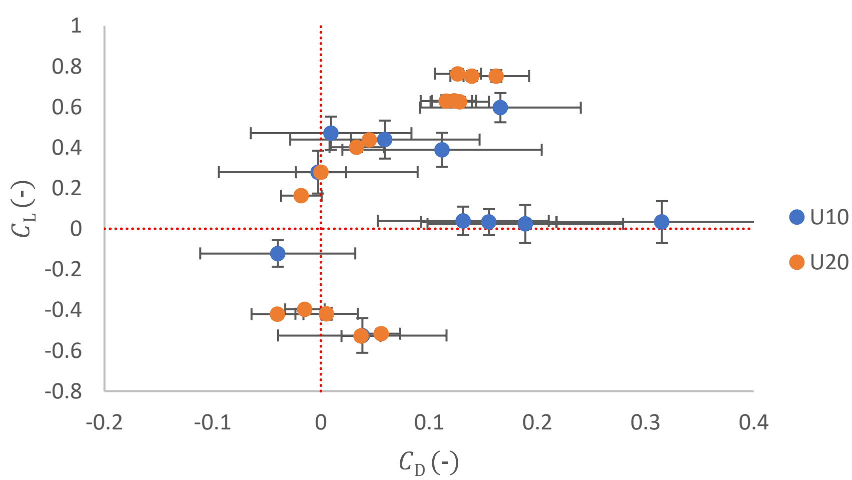

Figure 5 – Greater Reynolds number equated to a greater amount of drag and lift as shown above. Uncertainties were calculated for both drag and lift.

The lift/drag ratio vs. angle of attack provides insights into the aerodynamic efficiency of the airfoil. The ratio helps identify how well an airfoil performs by displaying how much lift the airfoil produces to the amount of drag it produces. The data points for my plot were skewed with extremely high uncertainties where the lift/drag ration was highest. This could be the result of an extremely low amount of drag resulting in lift to be an extremely high value. That being said, the plot does show a max lift/drag point for both the sets of initial velocities which is expected.

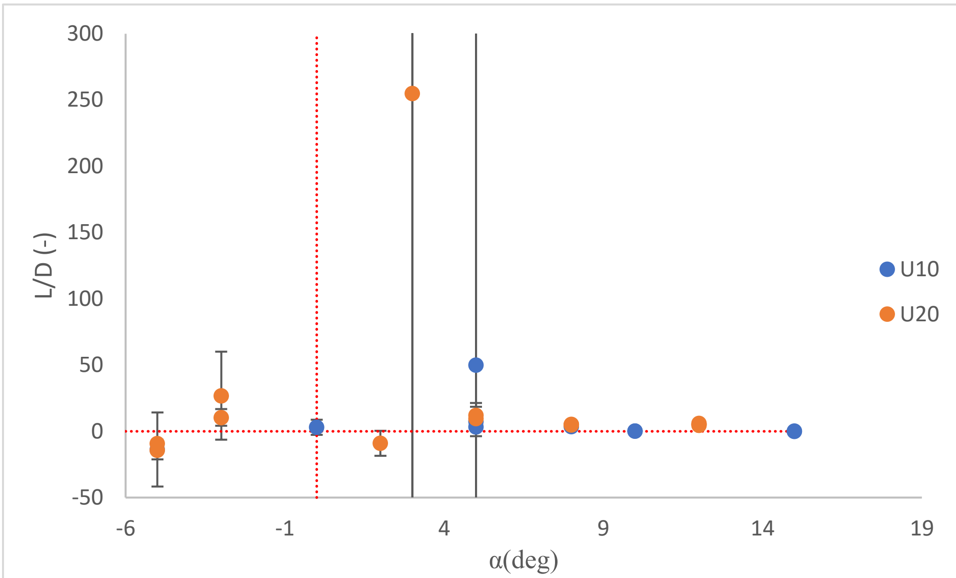

Figure 6 – Lift and drag ratio showed an extreme amount of uncertainty due to the lack of trails but showcases that at a higher Reynolds number there is a greater amount of efficiency.

To account for the wake velocity profile a momentum balance was taken where the blockage effect was considered and adjusted for using point-slop form. The original velocity profile and the new wake velocity profile were stabilized and subtracted from each other. This led to a linear more accurate plot. For the initial velocity of 10 [m/s], the moment balance characterized the drag coefficient with more linearity. Both methods line up well, indicating a congruence between the two methods. For the initial velocity of 20 [m/s] both the force balance and momentum balance approaches also line up. The momentum balance matches the scientific assumptions better than the force balance approach. At a higher Reynolds number, the coefficient of drag increased as shown in the both the figures below. Whereas at a lower Reynolds number, for the 10 [m/s] plot the coefficient of drag is less than at 20 [m/s]. For both velocities the momentum balance equation doesn't deviate below a zero coefficient of drag.

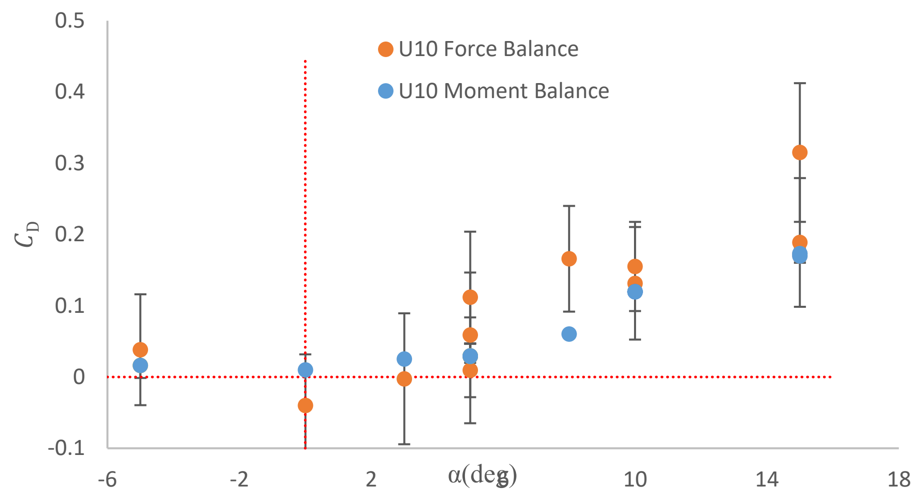

Figure 7 – The momentum and force balance approach combined plot for a 10 [m/s] velocity. The momentum balance approach displays a linear relationship between angle of attack and drag.

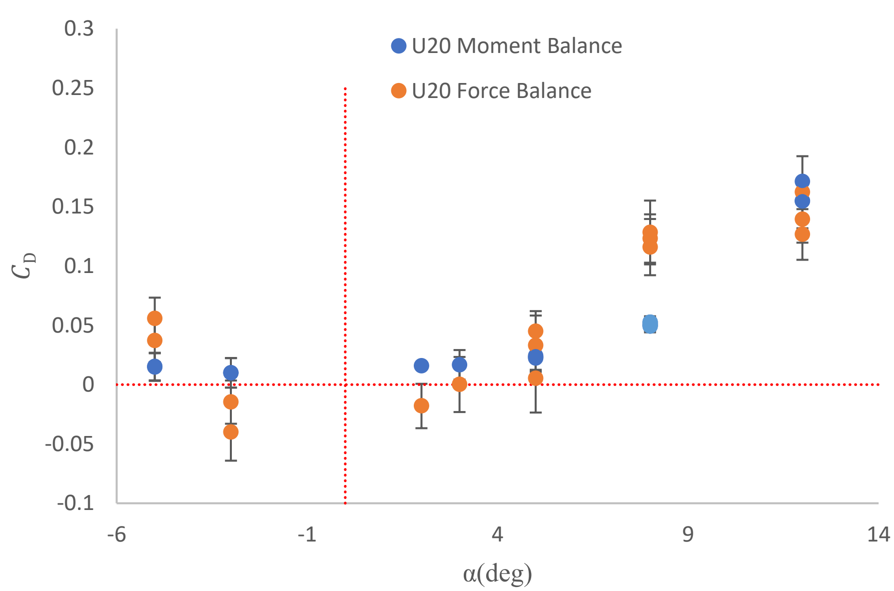

Figure 8 – The higher initial velocity led to a higher Reynolds number which in turn led to a greater amount of drag. This is proven by the momentum balance equation in the figure above.

Discussion/Conclusion

Results from both the momentum balance and force balance approach met the expectations of what was shown in class and what was written about in literature. However, the coefficient of drag vs. angle of attack plot using the force balance approach was skewed and did not show the appropriate relationship between an increase in Reynolds number with an increase in drag. This could have been due to the lack of trial data in the experiment. That being said, the coefficient of lift was greater at a Reynolds number of 122,000 ± 600 at 20 m/s instead of at 61,200 ± 1,100 at 10 m/s. The increase in lift with a higher Reynolds number theoretically should have led to an increase in efficiency, which it did but, the results were varied in the Figure 6, and the uncertainties were severely skewed possibly because of a very small drag coefficient in the data.

When comparing to the Selig paper, the NACA009 airfoil has a 9% thickness-to-chord ratio where as the NACA0010 used in this experiment had a 10% thickness-to chord-ratio. The increased thickness leads to greater lift at lower angles of attack. Comparing to our data, these results are in line and display similarities in lift coefficients and in the angle of attack. Granted the Reynolds number are not the same hence the slight discrepancies in values.

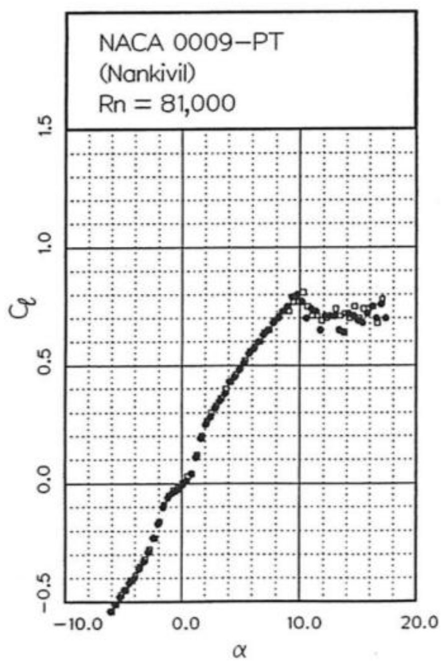

Figure 9 – Selig paper coefficients of lift results for NACA009 airfoil.

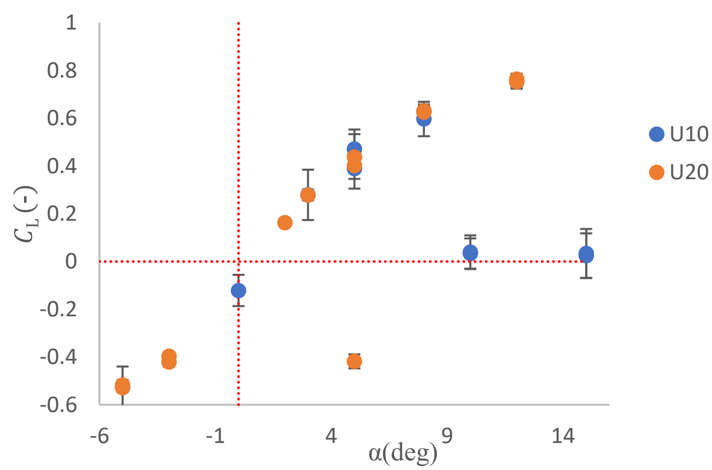

From aifoiltools.com, our data seemingly matched up to the results in the experiment. However, not enough data was captured to get the complete story. For the coefficients of drag vs. angle of attack plot there were negative values in the force balance equation but not in the momentum equation. Thus, the force balance equation does not line up with what was shown on the website.

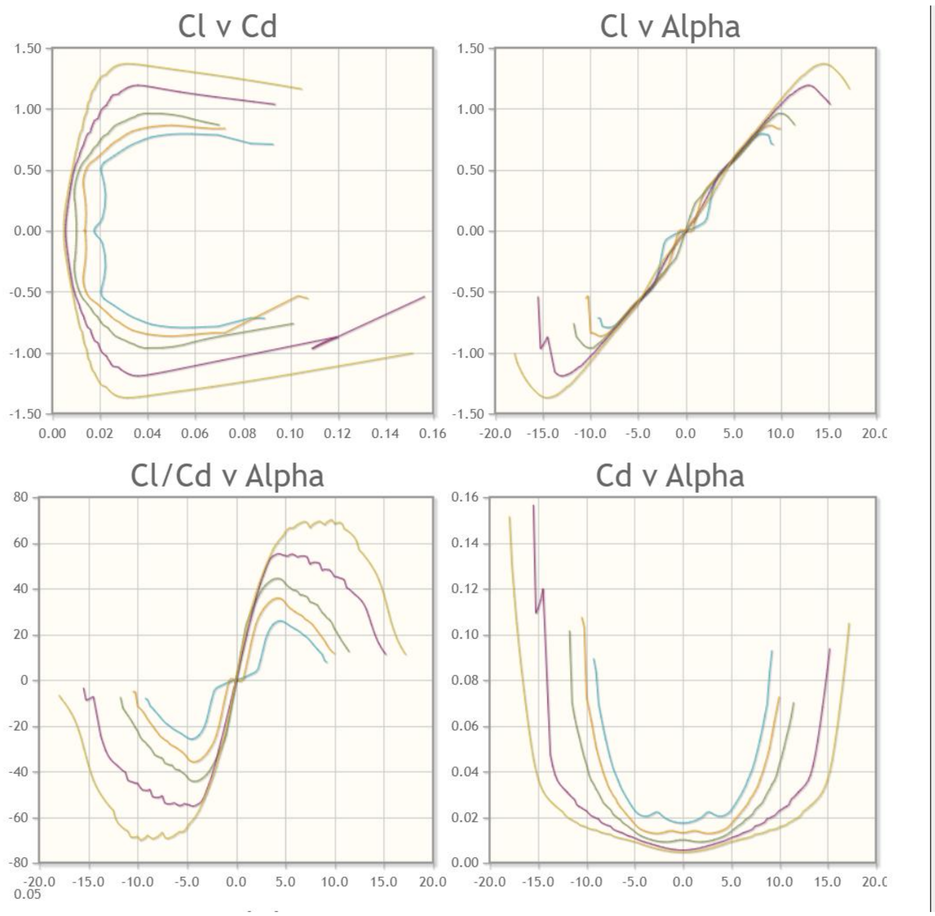

Figure 10 – data from airfoils.com of NACA0010 airfoil. The plots generally share the same shape albeit, with a lot more data.

Overall, the experiment proved that both the force balance approach and momentum balance approach were sufficient ways in characterizing an airfoil. However, a greater amount of trial sets and smaller increments of the angle of attack could have been beneficial in the overall results.

Citations

(1) NACA 0010 (NACA0010-IL). (n.d.). http://airfoiltools.com/airfoil/details?airfoil=naca0010-il

(2) Summary of low-speed airfoil data. (n.d.). https://m-selig.ae.illinois.edu/uiuc_lsat/Low-Speed-Airfoil-Data-V1.pdf